Folding and Homodimerization of Wheat Germ Agglutinin

María del Carmen Portillo-Téllez,[†] Martiniano Bello,[‡] Guillermo Salcedo,[†] Gabriel Gutiérrez,[†] Virginia Gómez-Vidales,[†] and Enrique García-Hernández[†*]

[†]Instituto de Química, Universidad Nacional Autónoma de México, Circuito Exterior, Ciudad Universitaria, México, D.F., México; and [‡]Instituto de Biotecnología, Universidad Nacional Autónoma de México, Cuernavaca, México

ABSTRACT Wheat germ agglutinin (WGA) is emblematic of proteins that specialize in the recognition of carbohydrates. It was the first lectin reported to have a capacity for discriminating between normal and malignant cells. Since then, it has become a preferred model for basic research and is frequently considered in the development of biomedical and biotechnological applications. However, the molecular basis for the structural stability of this homodimeric lectin remains largely unknown, a situation that limits the rational manipulation and modification of its function. In this work we performed a thermodynamic characterization of WGA folding and self-association processes as a function of pH and temperature by using differential scanning and isothermal dilution calorimetry. WGA is monomeric at pH 2, and one of its four hevein-like domains is unfolded at room temperature. Under such conditions, the agglutinin exhibits a fully reversible thermal unfolding that consists of three two-state transitions. At higher pH values, the protein forms weak, nonobligate dimers. This behavior contrasts with that observed for the other plant lectins studied thus far, which form strong, obligate oligomers, indicating a distinctly different molecular basis for WGA function. For dimer formation, the four domains must be properly folded. Nevertheless, depending on the solution conditions, self-association may be coupled with folding of the labile domain. Therefore, dimerization may proceed as a rigid-body-like association or a folding-by-binding event. This hybrid behavior is not seen in other plant lectins. The emerging molecular picture for the WGA assembly highlights the need for a reexamination of existing ligand-binding data in the literature.

INTRODUCTION

Metazoan cellular membranes are highly abundant in solvent-exposed glycoconjugates, collectively termed the glycocalyx. One of the glycocalyx's major roles is to serve as a sophisticated device for establishing cellular identity, and thus it is crucial for the discrimination between self and nonself. Additionally, the glycocalyx's composition varies significantly among different cell types and stages of differentiation. Thus, the study of proteins that are able to recognize membrane glycoconjugates with high specificity has proved invaluable for the development of drugs aimed at treating a wide number of diseases, including pathogenic infections, cancer, diabetes, and autoimmune disorders (1). Wheat germ agglutinin (WGA) was the first protein reported to have a capacity to discriminate between malignant and normal cells (2). Since then, this chitin-binding lectin has been used widely in biochemical and biomedical research (3–6). It is currently being considered as a candidate for peroral lectin-mediated drug delivery due to its mucoadhesion, cytoadhesion, cytoinvasive, and transcytosis properties with enterocytes (7,8). Promising results have also been obtained by using WGA in the direct delivery of drugs to the brain (9).

WGA forms homodimers at neutral pH that dissociate into compact monomers at low pH (10–12). Each subunit is composed of four domains (domains A–D) with a hevein-like fold. X-ray structures show the two subunits associated in a head-to-tail manner (13). Each subunit has four unique binding sites, one per domain. Hence, eight independent binding sites are present in the dimer, although because of the twofold symmetry axis, there are only four unique sites (14,15). Early solution-binding data indicated an occupancy of four sites per dimer (16–18). However, recent high-resolution structures have demonstrated that the eight binding sites are functional (19), as previously anticipated (15). It is worth noting that the existence of intercatenary binding sites in the WGA dimer contrasts markedly with the great majority of oligomeric lectins, whose binding sites are formed by residues coming from a single subunit.

Despite the numerous studies undertaken on WGA, the molecular basis for its stability and assembly is still largely unknown. It is recognized that this lectin, with 16 sulfide bridges per subunit, is very resistant to high temperature, caotropic agents, and acidic conditions (12,20). Nevertheless, its folding mechanism and energetics have not yet been determined. A quantitative description of the monomer/dimer equilibrium of WGA is also lacking (10,11). An understanding of the folding and homodimerization energetics as a function of pH would aid in guiding glycotargeting efforts with WGA. Furthermore, such information is crucial to clarify whether ligand binding is coupled to changes in the distribution of WGA monomers and dimers. In this study, we characterized the unfolding and dissociation energetics of WGA as a function of pH and temperature using high-precision differential scanning calorimetry (DSC) and isothermal dilution calorimetry (IDC). The results show that the folding of the free subunit is a multistep

Submitted June 3, 2011, and accepted for publication July 25, 2011.

*Correspondence: egarciah@unam.mx

Editor: Doug Barrick.

0006-3495/11/09/1423/9 $2.00

doi: 10.1016/j.bpj.2011.07.037

process, a behavior that correlates with the multidomain composition of the lectin. Furthermore, WGA forms weak transient homodimers. Depending on the solution conditions, dimerization may proceed (coupled or not) to significant conformational changes of the free subunits. This hybrid behavior is not seen in other plant lectins, indicating a different molecular basis for the function of WGA. Finally, we argue for the need to reexamine the carbohydrate-binding parameters reported for WGA, because the occurrence of coupled equilibria among dimerization and ligand binding to the free and dimeric subunits must be taken into account.

MATERIALS AND METHODS

Materials

WGA was purchased as a mixture of three isoforms (isoforms 1–3) from Sigma Chemical (L9640; St. Louis, MO). We separated the WGA isoforms by cationic exchange using high-performance liquid chromatography equipment, as previously described (12). All experiments were carried out using variant 1. All other reagents were of analytical quality. For measurements performed at pH values of 1.3, 2–3, 4–5, and 7, we used 30 mM buffer solutions of sulfate, glycine/HCl, acetate, and phosphate, respectively.

Fractions of purified WGA isoform 1 were concentrated and diafiltrated extensively in an Amicon-stirred cell through polyethersulfone ultrafiltration discs (cutoff 10 kD, PM10). Solutions were degassed exhaustively before the calorimetric experiments. Protein concentrations were determined spectrophotometrically with an absorption coefficient of 1.27 ml(mg cm)$^{-1}$ at 280 nm. The molecular mass of the WGA monomer was taken as 17.1 kDa.

Differential scanning calorimetry

DSC measurements were carried out with VP-DSC equipment (MicroCal, GE Health Bio-Sciences, Piscataway, NJ). All results presented were obtained at a scan rate of 60°C/h, although completely superimposable endotherms were obtained using a scan rate of 90°C/h. Buffer-buffer baselines were obtained under the same experimental conditions and subtracted from sample traces. We acquired several buffer-buffer baselines before each run with protein solution to obtain a proper thermal history of the instrument. Reheating runs were carried out to determine the calorimetric reversibility of the denaturation process. We fit the theoretical models to the heat capacity profiles using independent or sequential transition-unfolding models programmed in the MicroCal Origin v5 software package.

The van 't Hoff enthalpy (ΔH_{vH}) was calculated from calorimetric traces according to

$$\Delta H_{vH} = 4RT_{1/2}\frac{Cexc_{1/2}}{\Delta H_{cal}} \quad (1)$$

where R is the gas constant, $T_{1/2}$ is the mid-transition temperature, $Cexc_{1/2}$ is the heat capacity excess at this temperature, and ΔH_{cal} is the calorimetric enthalpy.

Isothermal dilution calorimetry

The dissociation of the WGA homodimer was characterized by IDC with VP-ITC equipment (MicroCal). Stepwise additions of small aliquots of a solution with a high protein concentration (0.7–1.2 mM of monomer equivalent) were applied to the calorimetric reaction cell loaded with buffer solution. According to a simple dimer dissociation model (21), the heat measured upon addition of the i^{th} injection of volume dV_i into the cell calorimeter would be

$$q_i = \Delta H_{disc}[P_2]_{syr}dV_i - \Delta H_{disc}\left([P_2]_i - [P_2]_{i-1}\right) \times \left(V_0 + \frac{dV_i}{2}\right) + q_{dil} \quad (2)$$

where ΔH_{disc} is the dissociation enthalpy of the dimer; $[P]$ and $[P_2]$ are the molar concentrations of the free monomer and dimer, respectively; and q_{dil} is the dilution heat of the protein. The dimer concentration in the reaction cell, $[P_2]_i$, and the syringe, $[P_2]_{syr}$, are in turn related to the corresponding equivalent monomer concentration, $[P_T]$, through the dissociation constant:

$$[P_T] = [P] + 2[P_2] = K_{disc}^{1/2}[P_2]^{1/2} + 2[P_2] \quad (3)$$

where K_{disc} is the equilibrium dissociation constant. ΔH_{disc} and K_{disc} were determined through a nonlinear regression fitting of Eqs. 2 and 3.

Fluorescence

Fluorescence spectra were recorded at 25°C in a PC1 spectrofluorometer equipped with a Peltier thermoelectric device (ISS, Champaign, IL) for temperature control. Protein samples of 3 μM of monomer were excited at 290 nm, and emission was collected from 310 to 410 nm.

Circular dichroism

Far-UV circular dichroism (CD) spectra were recorded on a JASCO J-720 spectropolarimeter (Jasco, Easton, MD) equipped with a Peltier thermoelectric device for temperature control. The instrument was calibrated with (+)-10-camphorsulfonic acid. Three scanning acquisitions were accumulated and averaged to yield the final spectrum. CD signals are reported as mean residue ellipticity, $[\Theta]_{mrw}$, using a value of 100 for the molecular weight of a mean residue.

Dynamic light scattering

DLS experiments were performed with a DynaPro-801 molecular sizing instrument (Protein Solutions, Chicago, IL) as described previously (22), using protein concentrations in the 0.1–0.4 mM range. The hydrodynamic radius (R_H) and the apparent molecular mass were estimated on the basis of an autocorrelation analysis of scattered light intensity data.

Changes in solvent-accessible surface area and structural-based estimation of heat capacity change

We carried out surface area calculations with the NACCESS program (S. J. Hubbard and J. M. Thornton, Department of Biochemistry and Molecular Biology, University College, London, 1993), using a probe radius of 1.4 Å and a slice width of 0.1 Å. Atomic coordinates of the WGA dimer isoform 1 were taken from the PDB file 2UVO (19). We generated the coordinates for the free subunits by simply erasing the coordinates of the other subunit, i.e., assuming a rigid-body-like association. Changes in solvent-accessible surface areas (ΔA) were estimated from the difference between the dimer and the sum of the free subunits. Changes in polar (ΔA_p) and apolar (ΔA_{ap}) surface areas were obtained from the change in accessible area of nitrogen/oxygen and carbon/sulfur atoms, respectively. We performed a structure-based calculation of the dimerization heat capacity using the empirical model:

$$\Delta Cp = 0.45(\pm 0.03)\,\Delta A_{ap} - 0.26(\pm 0.02)\,\Delta A_p \quad (4)$$

where the proportional coefficients, in cal mol^{-1} K^{-1} Å^{-2}, were obtained from dilution data of cyclic dipeptides (23).

RESULTS

Fig. 1 shows DSC endotherms of WGA obtained in the 2–7 pH range. Between pH 2 and 4, the unfolding process was reversible, as judged by the recovery of the endothermic signal ($\geq$90%) in protein samples previously submitted to a heating/cooling cycle. Similar results were observed by monitoring the far-UV CD signal (data not shown). The reversibility decreased to ~60% at pH 5, whereas no recovery of the calorimetric trace was observed at pH $\geq$ 6. Only one peak was evident at pH 2. This peak proved independent of protein concentration (Fig. 2 *A*), in agreement with previous sedimentation and spectroscopic results indicating that WGA is predominantly monomeric at that pH (10,12). As the pH was raised, an additional endothermic peak was observed at the lower temperatures. This peak was dependent on protein concentration (Fig. 2 *B*); therefore, it corresponds to the dissociation of the dimer. At pH 2.5, the use of low protein concentrations (e.g., 0.09 mM) yielded calorimetric traces that completely overlapped those obtained at pH 2, whereas the second peak became evident with the use of higher protein concentrations (e.g., 0.22 mM, as in Fig. 1).

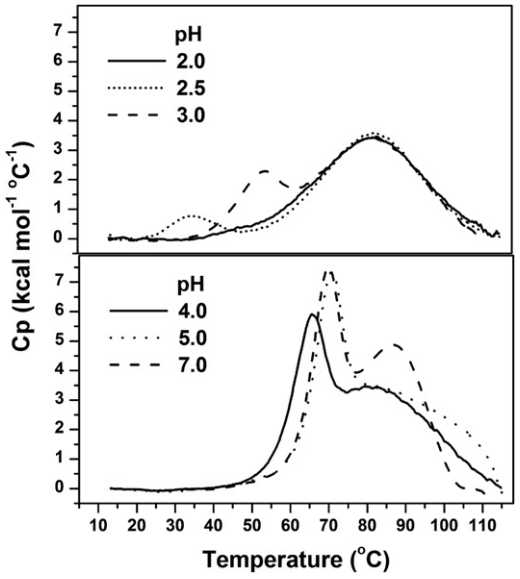

FIGURE 1 Calorimetric profiles of the thermal perturbation of WGA as a function of pH. All endotherms were obtained using a monomer equivalent concentration of 0.09 mM, except at pH 2.5, where a concentration of 0.22 mM was used. A heating rate of 1°C/min was used in all measurements. Complete recovery of the calorimetric trace was observed in the rescanning of a previously heated/cooled protein sample in solutions with pH $\leq$ 4. Reversibility at pH values of 5 and 7 were 60% and 0%, respectively.

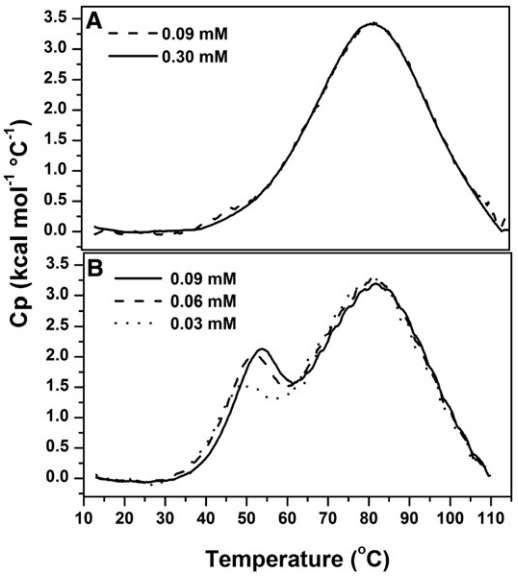

FIGURE 2 Calorimetric profiles of the thermal perturbation of WGA as a function of protein concentration at (*A*) pH 2 and (*B*) pH 3, 30 mM Gly/HCl.

Unfolding of monomeric WGA

The single endothermic peak obtained at pH 2 extended over a wide temperature range, suggesting the occurrence of stable intermediates in the unfolding process of monomeric WGA ($\Delta H_{vH}/\Delta H_{cal} = 0.3$). A deconvolution analysis revealed that the calorimetric traces can be fitted satisfactorily with a model of three independent two-state transitions. In contrast, models with any other number of transitions yielded poor fittings or failed to converge (see Fig. S1 in the Supporting Material). On the other hand, no significant differences in the unfolding parameters were obtained using a model of either sequential or independent unfolding transitions (Table S1). This result is most likely due to the fact that T_{mi} values are significantly separated from each other, implying, in practice, an independent character for the unfolding transitions. Consequently, Table 1 shows results for the unfolding parameters based on a mechanism of independent transitions.

The observation of only three calorimetric transitions, instead of the four expected according to the WGA domain composition, might be rationalized on the basis of different molecular scenarios. One possibility is that at pH 2, one domain is very stable and unfolds at temperatures higher than those reached in the calorimetric measurements. To explore this possibility, we carried out thermal scans in the presence of guanidine hydrochloride (GndHCl). Deconvolution analyses of these data yielded profiles that closely resembled that observed in the absence of the caotropic agent (Fig. S1), although the corresponding T_m and ΔH_U values were significantly decreased for the three transitions (Table 1). Again, no evidence of the fourth transition was

TABLE 1 Unfolding parameters for the calorimetric transitions of monomeric WGA, at pH 2 and varying concentrations of GndHCl

	Transition		
	1	2	3
		0 M GndHCl	
T_{mi} (°C)	68.0 ± 0.7	79.0 ± 0.6	91.1 ± 0.4
ΔH_{Ui} (kcal/mol)	31 ± 2	43 ± 3	42 ± 1
		1.5 M GndHCl	
T_{mi} (°C)	55.2 ± 0.2	69.4 ± 0.1	86.0 ± 0.3
ΔH_{Ui} (kcal/mol)	29 ± 1	40 ± 2	39 ± 1
		2 M GndHCl	
T_{mi} (°C)	52.6 ± 0.5	67.9 ± 0.3	81.9 ± 0.3
ΔH_{Ui} (kcal/mol)	28 ± 1	38 ± 1	36 ± 1

observed. Another scenario is that in highly acidic conditions, one domain becomes unstable but the contact with another domain suffices to keep it folded. Under this domain-domain coupling scenario, one transition would exhibit an unfolding enthalpy significantly higher than the other two transitions. When we use the reported experimental ΔCp value (= 0.56 kcal mol^{-1} K^{-1}) for hevein (24), extrapolation of unfolding enthalpies at 79°C (T_m for transition 2) yields 37.2 and 35.2 kcal mol^{-1} for transitions 1 and 3, respectively. These last values are comparable to that of transition 2 ($\Delta H_{U1} \approx \Delta H_{U3} \approx 0.85\Delta H_{U2}$). Furthermore, the unfolding parameters of each of the three calorimetric transitions are comparable to those reported for monomeric hevein under similar acidity conditions (T_m = 74°C, ΔH_U = 29 kcal mol^{-1}, pH = 2.1 (24)). Finally, interdomain coupling would be more readily affected by the caotropic agent. In contrast, both ΔH_U and T_m for each transition showed a linear dependence on GndHCl concentration (Fig. S2). Overall, the data do not seem to support the possibility that two of the hevein-like domains fold as a cooperative unit.

A third scenario for explaining the existence of only three unfolding transitions is that one of the domains is unstable and unfolded at pH 2. Fig. 3 *A* shows the fluorescence spectra of WGA measured in this study at different pH values. Although the protein dimerizes above pH 2, we recorded the spectra using a low protein concentration (3 μM), so only a minor fraction of monomers formed dimers at pH 4–5 (<6%; see below). The fluorescence intensity of the monomer at pH 2 is seen to be significantly lower than that exhibited at higher pH values. In this regard, it is relevant to recall an early study on CNBr-treated WGA (25). In that study, a WGA form cleaved at Met^{26}, i.e., near the middle of domain A, was obtained. This species was monomeric at neutral pH, exhibiting a decrease of ~30% in the fluorescence intensity. Of note, the acid monomer shows a quenching effect very similar to that observed in CNBr-treated WGA, with one domain disrupted. WGA has three Trp residues per subunit, at positions 41, 107, and 150, belonging to domains A, C, and D, respectively.

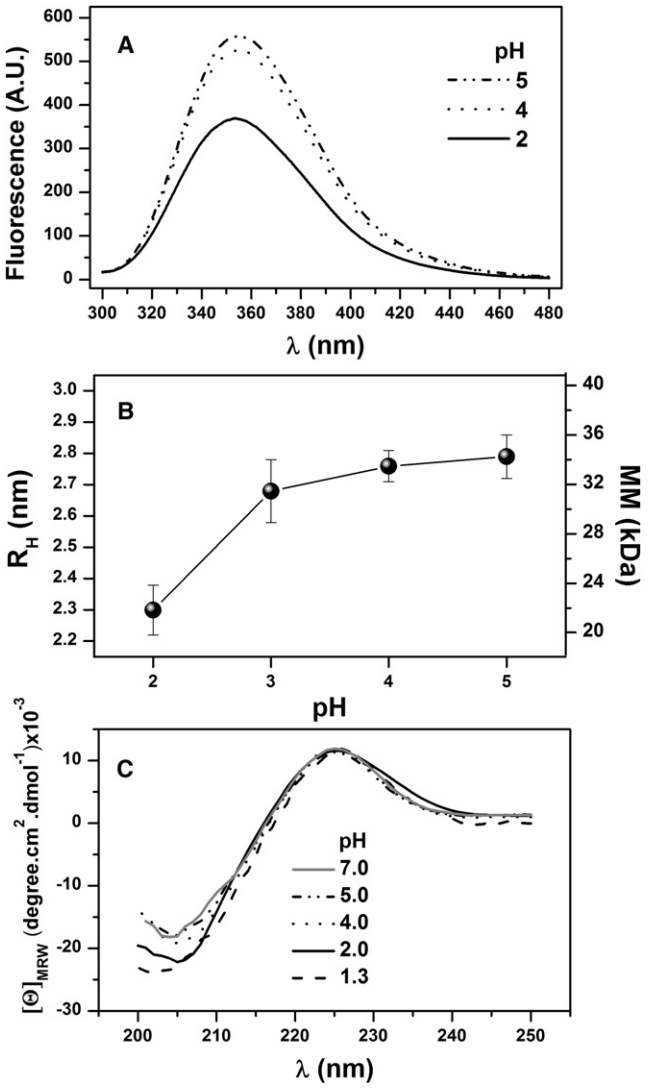

FIGURE 3 Spectroscopic properties of WGA at different pH values, 25°C. (*A*) Fluorescence spectra (λ_{exc} = 290 nm) obtained using a protein concentration of 3 μM. (*B*) Hydrodynamic radius and apparent molecular mass determined by DLS, using a protein concentration of 410 μM. (*C*) Far-UV CD spectra, recorded using protein concentration of 6 μM.

Thus, it seems likely that the quenching observed in intact WGA at pH 2 is also associated with a significant conformational change of one of the three Trp-containing domains. This conclusion is further supported by DLS results. As shown in Fig. 3 *B*, the acid monomer is somewhat expanded, showing an apparent molecular mass of 22 ± 2 kDa (versus the expected 17.1 kDa), whereas the corresponding value for the dimer at higher pH values averaged 33.7 kDa. On the other hand, the far-CD spectrum varied somewhat in the negative band centered at ~205 nm, as similarly observed in cleaved WGA (25). As can be seen in Fig. 3 *C*, this variation becomes more pronounced at pH 1.3, confirming that it is a distinguishing feature of the acid monomeric form of WGA. In summary, a global consideration of calorimetric and spectroscopic data suggests that the acid form of

WGA contains a partially unfolded domain that preserves a native-like content of secondary structure but a perturbed tertiary structure. Furthermore, this structural rearrangement was fully reversible, as evidenced by the fact that a sample previously incubated at pH 2 again attained the fluorescence enhancement seen in Fig. 3 *A* upon pH increase.

Unfolding and dissociation of dimeric WGA

As indicated above, DSC measurements taken at pH > 2 revealed the presence of an endothermic peak evolved from the dissociation of the dimer. As shown in Fig. 4 *A*, the temperature at which the dissociation peak reached its maximum ($T_{p,dis}$) increased significantly as pH was augmented. Thus, the dimer stabilizes as pH moves toward the isoelectric point of the lectin (pI = 7.3), although the stability seems to remain almost constant between pH 5 and 7. In contrast, the temperature at which the monomer unfolding peak reached its maximum ($T_{p,U}$) varied only slightly at pH $\leq$ 4, whereas it moved to higher temperatures at higher pH values, with a significant increase in the area under the peak, particularly at neutral pH. Nevertheless, under such conditions, the right side of the peak drops abruptly due to the exothermic effect accompanying the irreversible precipitation of the protein (Fig. 1).

To quantify WGA dimerization energetics, we carried out IDC measurements as a function of temperature and pH. Small aliquots of a high-concentration protein solution were added stepwise to the calorimeter cell loaded with buffer solution. The evolved heat signals are proportional to the dissociation enthalpy and the number of moles of dimers that dissociate upon dilution, which in turn depends on the dissociation constant and the total protein concentrations in the calorimeter syringe and reaction cell (Eqs. 2 and 3). The calorimetric data are well described with a dimer dissociation model, which includes the dilution heat of the protein as a fitting parameter (Fig. S3). Table 2 A summarizes the results of the IDC determinations at pH 3 as a function of temperature, in terms of dimer formation. Dimerization was enthalpically driven throughout the spanned temperature range. This favorable contribution was partially canceled out by an entropy decrease, except at 30°C (the lowest temperature assayed), where the entropy was favorable.

Fig. 5 shows the self-association enthalpy (ΔH_A) as a function of temperature. Two different trends can be distinguished in the plot. At lower temperatures ($T \leq 35$°C), ΔH_A varied linearly. In contrast, an increasingly more negative ΔCp_D was observed at higher temperatures. Considering only data between 30°C and 35°C, a heat capacity change (ΔCp_A) of -794 ± 8 cal mol^{-1} K^{-1} is obtained. Surface area-based calculations using the x-ray structure of WGA yielded dimeric interfacial polar and apolar areas of -1670 and -2630 Å^2, respectively. This area composition yields an interface hydropathy index ($\Delta A_p/\Delta A_t$) of 0.39, which is comparable to the average value observed in protein homodimers (26). According to Eq. 4, these changes are consistent with an expected ΔCp_A of -750 ± 57 cal mol^{-1} K^{-1}. It is worth noting that in the surface-area calculations, a rigid-body-like association behavior was assumed. Therefore, the good agreement between experimental and calculated ΔCp_A values indicates that below 35°C, WGA subunits self-associate without undergoing significant conformational changes. In contrast, the behavior observed above 35°C, in which an increasingly more negative ΔCp_A is apparent, typically is observed in protein complexes where at least one of the interacting molecules folds upon binding (27–29). In such cases, the observed energetics is a result of the pure binding plus the folding contributions. As temperature increases, a larger fraction of the free molecule becomes unfolded, thus yielding a larger apparent ΔCp_A. Indeed, consideration of both IDC and DSC results confirms that this is the case for WGA. As shown in Fig. 2 *B*, the onset of the unfolding processes occurs at approximately the temperature where thermal dependence of ΔCp_A is no longer linear. Therefore, it can be concluded that the low-temperature peak evident in DSC traces at pH $\geq$ 2.5 evolves from coupled dissociation and partial subunit unfolding heat effects.

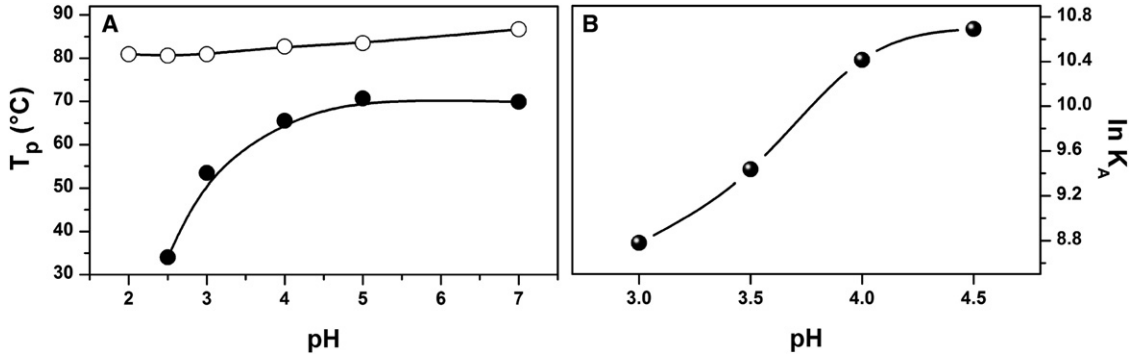

FIGURE 4 Stability of WGA as a function of pH. (*A*) Temperature at which the dissociation peak (*solid symbols*) and the monomer unfolding peak (*open symbols*) reach the maximum, as determined by DSC. (*B*) Dimerization equilibrium constant at 37°C, determined by IDC.

TABLE 2 Dimerization energetics of WGA measured by IDC

A. At pH 3, as a function of temperature

T (°C)	K_A ($M^{-1} \times 10^{-3}$)	ΔG_A (kcal mol^{-1})	ΔH_A (kcal mol^{-1})	$T\Delta S_A$ (kcal mol^{-1})
30	12.1 ± 0.2	−5.7	−3.4 ± 0.2	2.3
33	8.3 ± 0.5	−5.5	−5.8 ± 0.2	−0.3
35	7.3 ± 0.4	−5.5	−7.4 ± 0.4	−1.9
37	6.5 ± 0.3	−5.4	−9.6 ± 0.5	−4.2
40	6.2 ± 0.4	−5.4	−14.8 ± 0.2	−9.2
43	3.5 ± 0.7	−5.1	−23.6 ± 0.3	−18.5
46	0.8 ± 0.1	−4.3	−34.2 ± 3.1	−29.9

B. At 37°C, as a function of pH

pH	K_A ($M^{-1} \times 10^{-3}$)	ΔG_A (kcal mol^{-1})	ΔH_A (kcal mol^{-1})	$T\Delta S_A$ (kcal mol^{-1})
3.0	6.5 ± 0.3	−5.4	−9.6 ± 0.5	−4.2
3.5	12.5 ± 1.6	−5.8	−2.7 ± 0.1	3.1
4.0	33.3 ± 0.9	−6.4	−1.9 ± 0.1	4.5
4.5	44.0 ± 1.7	−6.6	−0.9 ± 0.1	5.7

IDC measurements were also carried out at a constant temperature (37°C) as a function of pH. Results for only the 3.0–4.5 pH range are presented (Table 2 *B*). Below this range, the interaction was too weak to be measured by IDC, whereas above pH 4.5, measurements were precluded due to low protein solubility and small heat signals. Although the dimer was enthalpically driven at pH 3, at higher pH values the entropic contribution became favorable and predominant. As shown in Fig. 4, the variation of K_A versus pH resembles that of $T_{p,dis}$. Therefore, DSC may be used as a convenient way to check the dimerization state of WGA. The curve shown in Fig. 4 *B* has a typical acid-base titration sigmoidal shape, with an apparent midpoint between pH 3.5 and 4.0. Free carboxylate groups in proteins usually have pKa values in this pH range. Inspection of the crystal structure of WGA (PDB 2UVO) reveals two pairs of equivalent acid residues (two residues per subunit) whose charged groups form part of the dimer interface: Asp^{86} and Glu^{115}. Each Glu^{115} is hydrogen-bonded to the hydroxyl group of Tyr^{37} at the other subunit, and forms part of a carbohydrate-binding site. In the case of Asp^{86}, each residue forms an intercatenary salt bridge with Arg^{84}. Of interest, the two pairs of intermolecular interactions are highly solvent-exposed. Thus, small pKa shifts may be expected for the corresponding carboxylate groups, consistent with the apparent pKa value observed in Fig. 4 *B*.

DISCUSSION

In this work, we used high-precision calorimetric techniques to characterize the stability and assembly mechanism of WGA isoform 1. The body of experimental data presented here indicates that dimer formation is a complex process that varies depending on the solution conditions. Subunit folding is a multistep process in which each of the four

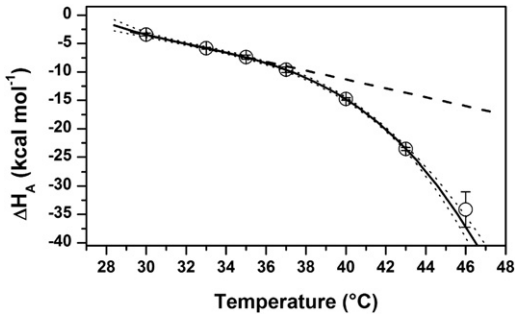

FIGURE 5 Dimerization enthalpy of WGA at pH 3 (50 mM Gly/HCl, 0.1 M NaCl) as a function of temperature. The solid line represents the best fitting of a third-order polynomial, which yields increasing ΔCp_A from −0.8 kcal mol^{-1} K^{-1} at 33°C to −5.5 kcal mol^{-1} K^{-1} at 46°C. The dotted line represents the best fitting of a straight line to data in the 30–35°C temperature range, with $\Delta Cp_A = -0.8$ kcal mol^{-1} K^{-1}.

hevein-like domains undergoes a two-state transition. Under conditions in which the free subunits have the four domains properly folded, dimerization proceeds following a rigid-body-like association. Acid- or thermal-induced unfolding of WGA domains efficiently opposes dimer formation. Nevertheless, there are some mild denaturation conditions in which the free subunit has a labile domain unfolded but the intermolecular contact is able to offset the energetic cost of the domain's folding. Under such circumstances, a folding-by-binding event takes place.

Self-association is a recurrent characteristic in a large number of plant lectins (30). In most cases, each protomer carries a single carbohydrate-recognition site. Therefore, homo-oligomerization is mandatory in these lectins to create the multisite scaffold that gives them the capacity for cell agglutination, a major defense mechanism in plants (6). The unfolding/dissociation processes of several homo-oligomeric plant lectins have been characterized thus far, mainly through chemical denaturation studies. Table 3 summarizes and compares the quaternary formation properties of these lectins. Most of these lectins have proven obligate oligomers, i.e., the subunits require quaternary structure formation to acquire the native conformation. In a sense, peanut lectin is an exception to this trend. This tetramer dissociates into compact monomers (31). Nevertheless, the free subunits adopt a molten-globule-like conformation, with reduced carbohydrate binding capacity (32). The lectins shown in Table 3 have considerably high structural stability, with coupled folding/oligomerization free energies of Gibbs ranging from −13 to −30 kcal mol^{-1} (dimer units). An exception to this is the case of frutalin, which shows a ΔG_A of only −6 kcal mol^{-1} (dimer units). Nonetheless, the actual stability of frutalin corresponds to that of the tetramer, as this oligomer forms from the unfolded free subunits in an all-or-none process (39). In fact, this formation mechanism and high structural stability are not surprising for proteins that require the oligomeric state to perform their biological activity.

TABLE 3 Formation mechanism and energetics of homo-oligomeric plant lectins

Lectin	Quaternary assembly*	ΔG_A† (kcal mol^{-1})	Temperature (°C)	pH	Ref.
Legume lectin					
Concanavalin A	4U $\rightarrow N_4$	−15	39	7.4	(33)
Concanavalin A	2U $\rightarrow N_2$	−16	35	5.0	(34)
Erythrina corallodendron lectin	2U $\rightarrow N_2$	−16	37	7.4	(35)
Erythrina indica lectin	2U $\rightarrow N_2$	−23	40	7.2	(36)
Pea lectin	2U $\rightarrow N_2$	−18	37	7.2	(37)
Peanut lectin	4I $\rightarrow N_4$	−15	37	7.4	(31)
Soybean agglutinin	4U $\rightarrow N_4$	−30	37	7.4	(33)
Winged bean acid lectin II	2U $\rightarrow N_2$	−13	35	5.0	(34)
Jacalin-related lectin					
Banana lectin	2U $\rightarrow N_2$	−18	25	7.0	(38)
Frutalin	4U $\rightarrow N_4$	−6	20	7.4	(39)

All data were determined from chemical denaturation assays.
*U, unfolded state; N, native state; I, folding intermediate state.
†Expressed in terms of mol of dimer.

At variance with the above lectins, WGA behaves as a weak, nonobligate homodimer. Although it was not possible to determine the dimer stability of WGA at neutral pH (as in most instances in Table 3), an inspection of Fig. 4 suggests a ΔG_A value close to −7 kcal mol^{-1}. This distinct behavior may imply that for the function of WGA, oligomerization is not as essential as it is for other plant lectins. In this context, it is relevant to mention the behavior observed for *Urtica dioica* agglutinin. This small protein is composed of two hevein-like domains, each of which possesses a carbohydrate-binding site (40). Thus, in spite of being monomeric, *U. dioica* agglutinin is able to agglutinate erythrocytes because its bidomain constitution. WGA could well behave likewise. Individual WGA domains have been shown to be binding competent (41). Thus, although self-association is crucial for WGA to attain maximum ligand affinity, the free monomers could also have significant activity. This situation would make dimerization less mandatory for WGA than for other oligomeric lectins with unicatenary recognition sites. On the other hand, it is worth recalling that several solution studies on the interaction of WGA with carbohydrates were carried out using relatively low protein concentrations. For instance, Bains et al. (18) used 30 μM WGA, pH 4.7, in their ITC measurements. According to dimerization constants in Table 2 *B*, in such experiments the fractions of subunits in monomeric and dimeric state could be similar to each other. Under such conditions, a complex equilibrium is taking place between ligand binding and lectin dimerization. Other binding studies on WGA (16,42–48) used lectin concentrations similar to or even smaller than those used by Bains et al. It follows then that a reexamination of the sugar-binding properties of WGA is needed.

At pH 2, where the agglutinin is monomeric, one of the domains is unfolded at room temperature. Further data are still required to identify which domain is unfolded, as well as to determine which structural domain corresponds to each transition detected in the DSC traces. To address this issue, we are currently in the process of expressing the isolated domains of WGA to characterize the individual folding energetics. This study will also help us ascertain whether interdomain folding cooperative effects are significant. In the meantime, it can be anticipated that domain B is one of the domains folded at pH 2. At variance with the other three domains, domain B is the only one that does not have any Trp residue. Therefore, it is less likely to be responsible for the fluorescence quenching observed at pH 2. Furthermore, sequence-based estimations (49) reveal that in going from pH 7 to pH 2, domain B has a smaller increase in its net electric charge (+1.2) as compared with domains C (+2.2), A (+3.2), and D (+4.2). Thus, the stability of domain B is presumably less compromised than that of the other three domains as the pH diminishes.

Regardless of which domain unfolds at low pH, this study shows that not only is the WGA monomer highly resistant to acidity, but that the conformational changes undergone by the lectin can be reversed by increasing pH. This property makes WGA highly suitable for peroral lectin-mediated drug delivery (7). In the stomach, the lectin would be present as a partially unfolded monomer. Binding experiments have shown that under such conditions, WGA binds poorly to pig gastric mucin (50). Thus, it is expected that the drug's vehicle will not be absorbed preferentially at this part of the gastrointestinal route. Once it reaches the intestine, an optimal zone for drug absorption, WGA will again attain its fully active conformation.

SUPPORTING MATERIAL

Three figures and one table are available at http://www.biophysj.org/biophysj/supplemental/S0006-3495(11)00895-2.

We thank Drs. Miguel Costas Basín (Facultad de Química, Universidad Nacional Autónoma de México (UNAM), México, D.F., México) and José Manuel Sánchez Ruiz (Facultad de Ciencias, Universidad de Granada, Granada, España) for the use of the VP-DSC calorimeter.

M.C.P.-T. received fellowships from the Consejo Nacional de Ciencia y Tecnología and Dirección General de Asuntos del Personal Académico during her graduate studies in the Programa de Doctorado en Ciencias Biomédicas, UNAM. This work was supported in part by the Dirección General de Asuntos del Personal Académico, UNAM (PAPIIT, grant IN204609) and Consejo Nacional de Ciencia y Tecnología (grant 129239).

REFERENCES

1. Sharon, N. 2008. Lectins: past, present and future. *Biochem. Soc. Trans.* 36:1457–1460.
2. Aub, J. C., B. H. Sanford, and M. N. Cote. 1965. Studies on reactivity of tumor and normal cells to a wheat germ agglutinin. *Proc. Natl. Acad. Sci. USA.* 54:396–399.

3. García, R., R. Rodríguez, …, J. A. Cremata. 1995. Concanavalin A- and wheat germ agglutinin-conjugated lectins as a tool for the identification of multiple N-glycosylation sites in heterologous protein expressed in yeast. *Anal. Biochem.* 231:342–348.
4. Leickt, L., M. Bergström, …, S. Ohlson. 1997. Bioaffinity chromatography in the 10 mM range of K_d. *Anal. Biochem.* 253:135–136.
5. Kilpatrick, D. C. 1999. Mechanisms and assessment of lectin-mediated mitogenesis. *Mol. Biotechnol.* 11:55–65.
6. Sharon, N., and H. Lis. 2004. History of lectins: from hemagglutinins to biological recognition molecules. *Glycobiology.* 14:53R–62R.
7. Gabor, F., E. Bogner, …, M. Wirth. 2004. The lectin-cell interaction and its implications to intestinal lectin-mediated drug delivery. *Adv. Drug Deliv. Rev.* 56:459–480.
8. Wood, K. M., G. M. Stone, and N. A. Peppas. 2008. Wheat germ agglutinin functionalized complexation hydrogels for oral insulin delivery. *Biomacromolecules.* 9:1293–1298.
9. Mistry, A., S. Stolnik, and L. Illum. 2009. Nanoparticles for direct nose-to-brain delivery of drugs. *Int. J. Pharm.* 379:146–157.
10. Nagata, Y., and M. M. Burger. 1974. Wheat germ agglutinin. Molecular characteristics and specificity for sugar binding. *J. Biol. Chem.* 249:3116–3122.
11. Rice, R. H., and M. E. Etzler. 1974. Subunit structure of wheat germ agglutinin. *Biochem. Biophys. Res. Commun.* 59:414–419.
12. Chavelas, E. A., A. P. Beltrán, …, E. García-Hernández. 2004. Spectroscopic characterization of the thermal unfolding of wheat germ agglutinin. *J. Mex. Chem. Soc.* 48:257–260.
13. Wright, C. S. 1987. Refinement of the crystal structure of wheat germ agglutinin isolectin 2 at 1.8 A resolution. *J. Mol. Biol.* 194:501–529.
14. Wright, C. S. 1992. Crystal structure of a wheat germ agglutinin/glycophorin-sialoglycopeptide receptor complex. Structural basis for cooperative lectin-cell binding. *J. Biol. Chem.* 267:14345–14352.
15. Wright, C. S., and G. E. Kellogg. 1996. Differences in hydropathic properties of ligand binding at four independent sites in wheat germ agglutinin-oligosaccharide crystal complexes. *Protein Sci.* 5:1466–1476.
16. Van Landschoot, A., R. G. Loontiens, …, C. K. De Bruyne. 1977. Binding of 4-methylumbelliferyl n-acetyl-chitooligosaccharides to wheat-germ agglutinin. A reinvestigation of equilibrium studies. *Eur. J. Biochem.* 79:275–283.
17. Kronis, K. A., and J. P. Carver. 1985. Wheat germ agglutinin dimers bind sialyloligosaccharides at four sites in solution: proton nuclear magnetic resonance temperature studies at 360 MHz. *Biochemistry.* 24:826–833.
18. Bains, G., R. T. Lee, …, E. Freire. 1992. Microcalorimetric study of wheat germ agglutinin binding to N-acetylglucosamine and its oligomers. *Biochemistry.* 31:12624–12628.
19. Schwefel, D., C. Maierhofer, …, V. Wittmann. 2010. Structural basis of multivalent binding to wheat germ agglutinin. *J. Am. Chem. Soc.* 132:8704–8719.
20. Rodríguez-Romero, A., B. Arreguín, and A. Hernández-Arana. 1989. Unusual far-ultraviolet circular dichroism of wheat germ agglutinin and hevein originated from cystine residues. *Biochim. Biophys. Acta.* 998:21–24.
21. Bello, M., M. D. Portillo-Téllez, and E. García-Hernández. 2010. Energetics of ligand recognition and self-association of bovine β-lactoglobulin: differences between variants A and B. *Biochemistry.* 50:151–161.
22. Arreguín-Espinosa, R., B. Fenton, …, E. García-Hernández. 2001. PFA, a novel mollusk agglutinin, is structurally related to the ribosome-inactivating protein superfamily. *Arch. Biochem. Biophys.* 394:151–155.
23. Murphy, K. P., and E. Freire. 1992. Thermodynamics of structural stability and cooperative folding behavior in proteins. *Adv. Protein Chem.* 43:313–361.
24. Hernández-Arana, A., A. Rojo-Domínguez, …, A. Rodríguez-Romero. 1995. The thermal unfolding of hevein, a small disulfide-rich protein. *Eur. J. Biochem.* 228:649–652.
25. Balasubramaniam, N. K., T. H. Czapla, and A. G. Rao. 1991. Structural and functional changes associated with cyanogen bromide treatment of wheat germ agglutinin. *Arch. Biochem. Biophys.* 288:374–379.
26. García-Hernández, E., R. A. Zubillaga, …, A. Hernández-Arana. 2000. Stereochemical metrics of lectin-carbohydrate interactions: comparison with protein-protein interfaces. *Glycobiology.* 10:993–1000.
27. Abian, O., J. L. Neira, and A. Velazquez-Campoy. 2009. Thermodynamics of zinc binding to hepatitis C virus NS3 protease: a folding by binding event. *Proteins.* 77:624–636.
28. Ladbury, J. E., and M. A. Williams. 2004. The extended interface: measuring non-local effects in biomolecular interactions. *Curr. Opin. Struct. Biol.* 14:562–569.
29. Freiburger, L. A., O. M. Baettig, …, A. K. Mittermaier. 2011. Competing allosteric mechanisms modulate substrate binding in a dimeric enzyme. *Nat. Struct. Mol. Biol.* 18:288–294.
30. Sinha, S., G. Gupta, …, A. Surolia. 2007. Subunit assembly of plant lectins. *Curr. Opin. Struct. Biol.* 17:498–505.
31. Dev, S., N. D. K, …, A. Surolia. 2006. Thermodynamic analysis of three state denaturation of peanut agglutinin. *IUBMB Life.* 58:549–555.
32. Reddy, G. B., V. R. Srinivas, …, A. Surolia. 1999. Molten globule-like state of peanut lectin monomer retains its carbohydrate specificity. Implications in protein folding and legume lectin oligomerization. *J. Biol. Chem.* 274:4500–4503.
33. Sinha, S., N. Mitra, …, A. Surolia. 2005. Unfolding studies on soybean agglutinin and concanavalin a tetramers: a comparative account. *Biophys. J.* 88:1300–1310.
34. Mitra, N., V. R. Srinivas, …, A. Surolia. 2002. Conformational stability of legume lectins reflect their different modes of quaternary association: solvent denaturation studies on concanavalin A and winged bean acidic agglutinin. *Biochemistry.* 41:9256–9263.
35. Mitra, N., N. Sharon, and A. Surolia. 2003. Role of N-linked glycan in the unfolding pathway of *Erythrina corallodendron* lectin. *Biochemistry.* 42:12208–12216.
36. Ghosh, S., and D. K. Mandal. 2006. Kinetic stability plays a dominant role in the denaturant-induced unfolding of *Erythrina indica* lectin. *Biochim. Biophys. Acta.* 1764:1021–1028.
37. Ahmad, N., V. R. Srinivas, …, A. Surolia. 1998. Thermodynamic characterization of the conformational stability of the homodimeric protein, pea lectin. *Biochemistry.* 37:16765–16772.
38. Gupta, G., S. Sinha, and A. Surolia. 2008. Unfolding energetics and stability of banana lectin. *Proteins.* 72:754–760.
39. Campana, P. T., D. I. Moraes, …, L. M. Beltramini. 2002. Unfolding and refolding studies of frutalin, a tetrameric D-galactose binding lectin. *Eur. J. Biochem.* 269:753–758.
40. Harata, K., and M. Muraki. 2000. Crystal structures of *Urtica dioica* agglutinin and its complex with tri-N-acetylchitotriose. *J. Mol. Biol.* 297:673–681.
41. Espinosa, J. F., J. L. Asensio, …, J. Jiménez-Barbero. 2000. NMR investigations of protein-carbohydrate interactions binding studies and refined three-dimensional solution structure of the complex between the B domain of wheat germ agglutinin and N,N′, N″-triacetylchitotriose. *Eur. J. Biochem.* 267:3965–3978.
42. Privat, J.-P., and M. Monsigny. 1975. Luminescence studies of saccharide binding to wheat germ agglutinin (lectin). *Eur. J. Biochem.* 60: 555–567.
43. Thomas, M. W., E. F. Walborg, Jr., and B. Jirgensons. 1977. Circular dichroism and saccharide-induced conformational transitions of wheat germ agglutinin. *Arch. Biochem. Biophys.* 178:625–630.
44. Clegg, R. M., F. G. Loontiens, …, T. M. Jovin. 1983. Dynamic evidence for an extended subsite structure of the ligand combining site on wheat germ agglutinin: temperature-jump relaxation with fluorescence detection. *Biochemistry.* 22:4797–4804.

45. Nagahora, H., K. Harata, …, Y. Jigami. 1995. Site-directed mutagenesis and sugar-binding properties of the wheat germ agglutinin mutants Tyr73Phe and Phe116Tyr. *Eur. J. Biochem.* 233:27–34.

46. Kristiansen, A., Å. Nysæter, …, K. M. Vårum. 1999. Quantitative studies of the binding of wheat germ agglutinin (WGA) to chitin-oligosaccharides and partially *N*-acetylated chitosans suggest inequivalence of binding sites. *Carbohydr. Polym.* 38:23–32.

47. Muraki, M., M. Ishimura, and K. Harata. 2002. Interactions of wheat-germ agglutinin with GlcNAc β 1,6Gal sequence. *Biochim. Biophys. Acta.* 1569:10–20.

48. Bogoeva, V. P., M. A. Radeva, …, R. N. Boteva. 2004. Fluorescence analysis of hormone binding activities of wheat germ agglutinin. *Biochim. Biophys. Acta.* 1698:213–218.

49. Bjellqvist, B., G. J. Hughes, …, D. Hochstrasser. 1993. The focusing positions of polypeptides in immobilized pH gradients can be predicted from their amino acid sequences. *Electrophoresis.* 14:1023–1031.

50. Irache, J. M., C. Durrer, …, G. Ponchel. 1994. In vitro study of lectin-latex conjugates for specific bioadhesion. *J. Control. Release.* 31:181–188.